Published in final edited form as:
Nucl Med Biol. 2014 July ; 41(6): 441–449. doi:10.1016/j.nucmedbio.2014.03.026.

Radiolabeling and in vitro evaluation of ^{67}Ga-NOTA-modular nanotransporter – A potential Auger electron emitting EGFR-targeted radiotherapeutic

Eftychia Koumarianou[a], **Tatiana A. Slastnikova**[b,c], **Marek Pruszynski**[a,d], **Andrey A. Rosenkranz**[b,c], **Ganesan Vaidyanathan**[a], **Alexander S. Sobolev**[b,c], and **Michael R. Zalutsky**[a,e,*]

[a]Department of Radiology, Duke University Medical Center, Durham, NC, USA

[b]Laboratory of Molecular Genetics of Intracellular Transport, Institute of Gene Biology, Moscow, Russia

[c]Department of Biophysics, Moscow State University, Moscow, Russia

[e]Departments of Biomedical Engineering and Radiation Oncology, Duke University, Durham, NC, USA

Abstract

Introduction—Modular nanotransporters (MNTs) are vehicles designed to transport drugs from the cell surface via receptor-mediated endocytosis and endosomal escape to nucleus. Hence their conjugation to Auger electron emitters, can cause severe cell killing, by nuclear localization. Herein we evaluate the use of MNT as a platform for targeted radiotherapy with ^{67}Ga.

Methods—EGF was the targeting ligand on the MNT, and NOTA was selected for its radiolabeling with ^{67}Ga. In the radiolabeling study we dealt with the precipitation of MNT (pI 5.7) at the labeling pH (4.5–5.5) of ^{67}Ga. Cellular and nuclei uptake of ^{67}Ga-NOTA-MNT by the A431 cell line was determined. Its specific cytotoxicity was compared to that of ^{67}Ga-EDTA, ^{67}Ga-NOTA-BSA and ^{67}Ga-NOTA-hEGF, in A431 and U87MGWTT, cell lines, by clonogenic assay. Dosimetry studies were also performed.

Results—^{67}Ga-NOTA-MNT was produced with 90% yield and specific activity of 25.6 mCi/mg. The *in vitro* kinetics revealed an increased uptake over 24 h. 55% of the internalized radioactivity was detected in the nuclei at 1 h. The cytotoxicity of ^{67}Ga-NOTA-MNT on A431 cell line was 17 and 385-fold higher when compared to non-specific ^{67}Ga-NOTA-BSA and ^{67}Ga-EDTA. While its cytotoxic potency was 13 and 72 – fold higher when compared to ^{67}Ga-NOTA-hEGF in the A431

*Corresponding author: Duke University Medical Center, Box 3808, Durham, NC 27710 USA. Tel: +1 919 684 7708, fax: +1 919 684 7121. zalut001@mc.duke.edu (M.R. Zalutsky).
[d]Present address: Institute of Nuclear Chemistry and Technology, Warsaw, Poland

and the U87MGWTT cell lines, respectively, validating its nuclear localization. The absorbed dose, for 63% cell killing, was 9 Gy, confirms the high specific index of ^{67}Ga.

Conclusion—These results demonstrate the feasibility of using MNT as a platform for single cell kill targeted radiotherapy by Auger electron emitters.

Keywords

^{67}Ga; Auger electron emitter; modular nanotransporter; radionuclide therapy; EGFR

1. Introduction

Because most Auger electrons have tissue path lengths <0.1 μm, their cytotoxic effectiveness is critically dependent on the subcellular decay site of radionuclides emitting this type of radiation. Auger electron-emitters exert their radiotoxic effects mainly when internalized into cancer cells, more so when imported into the cell nucleus and most effectively when tightly bound to DNA, where they can cause highly cytotoxic DNA double-strand breaks [1]. Nonetheless, there are reports suggesting that localization of Auger electrons in the close proximity of DNA is not necessary for cytotoxic effectiveness [2,3]. On the other hand, the highly targeted toxicity of Auger electron emitters through cell internalization could minimize the nonspecific radiotoxicity frequently observed with β-emitters [4,5], which could be of particular importance for killing isolated cancer cells.

Comparing the effect of subcellular localization on the dose delivered by different Auger electron emitters to the radiation-sensitive cell nucleus needs to take into account differences in their electron emission spectra [2], which can be accomplished conveniently using subcellular S-value tables [6]. If one considers a cell with a radius of 10 μm and nuclear radius of 7 μm, then with the prototypical Auger electron emitter ^{125}I moving the site of decay from the cell membrane to the nucleus would increase the radiation dose delivered to the cell nucleus by 18.9 and with ^{67}Ga, the advantage imparted by nuclear translocation is even higher – 33.8. Thus, molecules that can enable both selective and efficient delivery of Auger emitters to the nucleus of cancer cells are an essential component of Auger -electron targeted radiotherapy strategies.

With that goal in mind, we have created modular nanotransporters (MNT), an engineered recombinant polypeptide that includes domains for accomplishing receptor binding, internalization, endosome escape and nuclear import, enabling delivery of radionuclides from the cell surface to the nucleus [7]. A somewhat similar concept that has been investigated recently is the conjugation of multiple nuclear localization sequence (NLS) peptides to an internalizing antibody (mAb) [8,9]. Although NLS conjugation enhanced nuclear localization, most of the radioactivity was found in other cellular compartments. In addition to their smaller size, a potential advantage of MNT compared with mAb-NLS conjugates, is the presence of an endosome escape module, which should increase the probability of interaction of the NLS with cytoplasmic importins, thereby facilitating nuclear translocation. The 76.3-kDa MNT used in the present study contained epidermal growth factor (EGF) as the ligand module to be able to target the multiple malignancies including breast cancer and glioblastoma that overexpress EGF receptors (EGFR) [10,11]. Previous

studies established that this MNT was highly effective in enhancing the cytotoxicity of short range of action photosensitizers [12,13] and α-particles [7] against EGFR-expressing cancer cells. Moreover, we have recently demonstrated the potential utility of MNT as a delivery platform for Auger electron emitters in proof of principle studies with ^{125}I using the residualizing prosthetic agent *N*-succinimidyl 4-guanidinomethyl-3-[^{125}I]iodobenzoate ([^{125}I]SGMIB) [14].

The objective of the current study was to extend this strategy to evaluate an Auger electron emitter with characteristics more amenable to clinical translation. Gallium-67 was chosen for this purpose based on its shorter half life (3.3 d), higher nuclear enhancement factor (*vide supra*) and availability of bifunctional chelators with excellent properties for use with gallium radionuclides [15]. Herein, we present results for labeling MNT with ^{67}Ga via *S*-2-(4-isothiocyanatobenzyl)-1,4,7-triazacyclononane-1,4,7-triacetic acid (p-SCN-Bn-NOTA) as well as the *in vitro* evaluation of ^{67}Ga-NOTA-MNT on EGFR-expressing human cancer cell lines.

2. Material and Methods

2.1 Chemicals

All chemicals were purchased from commercial sources and used without additional purification. p-SCN-Bn-NOTA was purchased from Macrocyclics (Dallas, TX) and used as received. [^{67}Ga]Gallium chloride was obtained from Nordion (Vancouver, Canada) with a specific activity >1000Ci/g and a radioactive concentration of 1350 mCi/mL in 0.05 N HCl. The anion exchange resin Accell Plus CM QMA was obtained from Waters (Milford, MA).

2.2 Modular nanotransporter

Construction, purification and validation of module function of this MNT were as described [16]. In this MNT, the translocation domain of diphtheria toxin served as the endosome escape module, an *Escherichia coli* hemoglobin-like protein served as the carrier module, the optimized SV40 large T-antigen NLS peptide was included for nuclear import and EGF served as the ligand module. The MNT isoelectric point is 5.7, which resulted in its precipitation at concentrations higher than 4–5 mg/mL at pH between 3.5 and 7.4, confounding its radiolabeling.

2.3 Conjugation of MNT to p-SCN-Bn-NOTA

All buffers used were prepared using procedures designed to minimize adventitious metal ion contamination. The NOTA-MNT conjugate was prepared by incubating 3–5 mg MNT with a 23-fold molar excess of p-SCN-Bn-NOTA in 1× pH 8.6 conjugation buffer [17] for 24 h at 20–25°C with final concentrations of MNT ≥0.25 mg/mL. The conjugate was concentrated and separated from excess chelator using a 10-kDa cutoff Centricon® concentrator (Amicon Ultra, Millipore, Billerica, MA). During this process, the conjugation buffer was gradually replaced with Dulbecco's phosphate-buffered saline (DPBS; Ca/Mg-free; pH 7.4). The number of chelates per MNT (Chelate/Biomolecule, C/B) was determined by the matrix-assisted laser desorption ionization mass spectroscopy (MALDI-MS) performed on a Voyager-DE PRO BioSpectrometry workstation (Applied Biosystems,

Grand Island, NY) using a nitrogen laser at 347 nm with 20 shots per second, and analyzing the data with Data Explorer version 5.1 software. The final concentration of NOTA-MNT was determined using the Bradford protein assay (BioRad, Grand Island, NY). The NOTA-MNT conjugate along with unmodified MNT were analyzed under non-reducing conditions by SDS-PAGE using Mini-PROTEAN TGX Any kD gels (BioRad, Grand Island, NY). For comparison purposes in the cytotoxicity assays, human epidermal growth factor (hEGF) and bovine serum albumin (BSA) were also conjugated with p-SCN-Bn-NOTA following the above protocol.

2.4 Labeling NOTA-MNT with ^{67}Ga

The labeling of NOTA-MNT with ^{67}Ga was evaluated with regard to yield and achievable specific activity. Variables investigated were pH (buffers: pH 3.5, 0.15 M sodium citrate; pH 5.0, 0.5 M NH_4OAc; pH 8.2, 0.6 M $NaHCO_3$), time (15, 30, 60 and 120 min), and temperature (20°C and 37°C). After optimization, the conditions employed for labeling MNT for the *in vitro* experiments were as follows: Gallium-67 (0.5 to 3.0 mCi in 2–4 μL of 0.05 M HCl) was diluted with 0.5 M NH_4OAc buffer, pH 5.0, to a final volume of 100 μL in an Ependorff tube. NOTA-MNT (100 μg/50 μL DPBS) was added and diluted to a final volume of 200 μL. Gentle shaking of the mixture resulted in the precipitation of NOTA-MNT. The heterogeneous mixture was incubated at 37°C for 1 h, without agitation, and then centrifuged at 12500 rpm for 2–3 min. The supernatant was removed and 400 μL of 0.2 M Na_2HPO_4/0.2 M NaH_2PO_4, pH 8.0 buffer and 20 μL dimethyl sulfoxide (DMSO) was added to the pellet. Colloidal ^{67}Ga present in the mixture was separated by centrifugation and the supernatant was passed through a Sephadex G25 PD-10 column (GE Healthcare, Piscataway, NJ) eluted with DPBS. Radiolabeling of NOTA-BSA and NOTA-hEGF was performed as follows: 0.5–3.0 mCi of ^{67}Ga in 2–4 μL 0.05 M HCl was diluted with pH 5.0 0.5 M NH_4OAc buffer to 100 μL in an Ependorff tube, and 50–100 μg of the NOTA conjugate in DPBS was added, and diluted to a final volume of 200 μL with 0.5 M NH_4OAc. The sample was gently stirred and then incubated for 1 h at 37°C without agitation. The ^{67}Ga-NOTA conjugates were purified by gel filtration over a Sephadex G25 PD-10 column.

2.5 Determination of radiolabeling yield

Labeling yields were determined by silica gel instant thin layer chromatography (ITLC-SG, Gelman Science, MI) using 0.1 M citric acid as the mobile phase. The ^{67}Ga-NOTA-MNT remained at origin and free ^{67}Ga migrated with the solvent front. The radiolabeling yield was also determined before and after PD-10 column purification by methanol precipitation as described [18]. SDS-PAGE analysis was performed under non-reducing conditions on samples before and after PD-10 column purification. Radioactivity on dried gels was detected using a phosphor imager (Cyclone Plus, Perkin-Elmer, Dowbers Grove, IL). The obtained images were analyzed using OptiQuant Version 5.0 software.

2.6 In vitro studies

2.6.1 Cell lines and culture conditions—Two cell lines were used in this study. The A431 human epidermoid carcinoma cell line was obtained from ATCC (CRL-1555™,

Manassas, VA) and the human glioblastoma cell aline U87MGwtEGFR (hereafter referred to as WTT) was kindly provided by Darell Bigner, Department of Pathology, Duke University Medical Center. The WTT cell line was derived from the U87MG cell line by transfecting it with the wild-type EGFR gene [19]. Both cell lines were cultured in Improved MEM Zinc Option medium (Gibco, Grand Island, NY) supplemented with 10% fetal bovine serum (FBS; Gibco, Grand Island, NY), streptomycin 100 μg/mL, and penicillin 100 U/mL (Sigma Aldrich, St. Louis, MO). Cells were maintained in a humidified atmosphere with 5% CO_2 at 37°C and fed every 2 days and sub-cultured by trypsinization (0.25% Trypsin-EDTA for A431 and 0.05% Trypsin-EDTA for WTT, Gibco, Grand Island, NY), when the cells have covered about 80% of the surface in the flask.

2.6.2 Uptake and washout kinetics—The uptake of ^{67}Ga-NOTA-MNT by A431 cells *in vitro* was studied as a function of time. Briefly, the cells were seeded in 24-well plates (5×10^4 cells/well) and 48 h later, the cells were incubated with ^{67}Ga-NOTA-MNT (5.7 nM) in triplicate for 0.5, 1, 2, 4, 8, 12 and 24 h at 37°C in a 5% CO_2 humidified atmosphere. Nonspecific uptake was determined at 2 h by coincubation with a 100-fold molar excess of hEGF. Unbound radioactivity-containing medium was collected at each time point and the cells were washed with ice cold DPBS, trypsinized, harvested, and pelleted by centrifugation. The pelleted cells were washed further, pelleted again, and the supernatants were combined with previous ones. The internalized (pelleted cells), membrane-bound (supernatant after centrifugation) and the unbound radioactivity (supernatant before trypsinization), were counted for ^{67}Ga using the automated gamma counter. To determine washout kinetics, A431 cells were incubated with 5.7 nM of ^{67}Ga-NOTA-MNT for 24 h in a 5% CO_2 humidified atmosphere at 37°C. After trypsinization and washing, the cells were resuspended in media, and incubated for 0.5, 2, 4, 8, and 24 h, each in triplicate, in a 5% CO_2 humidified atmosphere at 37°C. The washed out radioactivity was removed by centrifugation, followed by an additional washing of the cells with medium and centrifugation. After ^{67}Ga counting, results were expressed as cpm of internalized radioactivity per cell as a function of time. Two independent experiments were performed for each assay.

2.6.3 Nuclear kinetics—To evaluate the extent of ^{67}Ga accumulation in cell nuclei, a nuclear kinetics assay was performed using a widely used method for the isolation of nuclei [20]. Briefly, A431 cells were seeded in 6-well plates (5×10^5 cells/well) and 2 days later, the cells were washed and incubated in triplicate with 12 nM of ^{67}Ga-NOTA-MNT for 1, 2, 4, 8 and 24 h in a 5% CO_2 humidified atmosphere at 37°C. For the determination of nonspecific uptake, a 100-fold molar excess of hEGF also was added to cells at the 2 h time point. Unbound radioactivity containing medium was collected at each time point and the cells were washed three times with 1 mL of ice-cold DPBS. The cells were trypsinized and harvested for centrifugation. The supernatant containing the membrane-bound radioactivity (released by trypsinization) was collected and the cells were washed with ice-cold medium. The washings were combined with the initial supernatants. The cells were swelled for 20 min on ice in 500 μL of ice-cold hypotonic buffer (25 mM Tris-HCl pH 7.5, 5 mM KCl, 0.5 mM dithiothreitol (DTT), 1 mM phenylmethanesulfonylfluoride (PMSF), and 0.15 U/mL aprotinin) and, to determine intracellular radioactivity, 50 μL aliquots were removed and

counted. Following homogenization using a Dounce homogenizer (15 strokes) on ice, the nuclei were pelleted by centrifugation at 600 × g for 10 min at 4°C. Pelleted nuclei were washed three times with 500 μL of ice-cold isotonic buffer (0.25 M sucrose, 6 mM $MgCl_2$, 10 mM Tris-HCl, pH 7.4, 0.5% Triton X-100, 1 mM PMSF, and 0.15 U/mL aprotinin) to remove any contamination from cytoplasmic membranes. The pelleted nuclei fractions were re-suspended in DPBS and examined for their purity and yield of nuclei by microscopic evaluation in a hematocytometer. The radioactivity in the samples was counted and the results were expressed as cpm/cell, cpm/nucleus, and percent of total cell-associated radioactivity as a function of time. The purity of isolated nuclei was evaluated by Western Blot analysis using antibodies to α-tubulin (cytoplasmic marker) and histone deacetylase-1 (HDAC-1) (nuclear marker) as described [20].

2.6.4 Cytotoxicity study—The *in vitro* cytotoxicity of ^{67}Ga-NOTA-MNT and ^{67}Ga-NOTA-hEGF was evaluated on both A431 and WTT cells. In addition, ^{67}Ga-EDTA and ^{67}Ga-NOTA-BSA were studied only with the A431 cell line to assess nonspecific cytotoxicity. Briefly, cells were seeded in 24-well plates (5×10^4 cells/well) and 2 days later, were incubated with increasing radioactive concentrations of each compound in a 5% CO_2 humidified atmosphere at 37°C for 24 h. Protein-associated ^{67}Ga activity in the cell culture media was determined by methanol precipitation. Unbound radioactivity-containing medium was removed and the cells were washed twice with cold DPBS, trypsinized and harvested. After centrifugation, the supernatant, representing membrane-bound radioactivity, was collected. The cells were resuspended in medium and an aliquot was collected in order to count the amount of internalized radioactivity. Cells suspensions (1 mL) containing 2000 A431 cells or 10000 WTT cells were seeded in triplicate into 25-cm^2 flasks containing 4 mL of cell culture medium. After 6–7 d (A431 cells) or 14 d (WTT cells), colonies were stained and counted; colonies comprising 50 or more cells were scored as viable. The results were plotted as percent survival as a function of added radioactivity concentration. Two independent experiments for each of the compounds were performed.

2.7 Calculation of decays per cell and cell nucleus

The total number of ^{67}Ga cpm delivered to the cells during the cytotoxicity experiment was calculated from the curves obtained for internalized cpm uptake and washout over time. These calculations were done utilizing the formulae for calculating the number of decays occurring inside the cell and the cell nucleus previously utilized to analyze the results of similar assays performed with ^{125}I-MNT [14]. They were adapted for use with ^{67}Ga by substituting a value of 0.70 for *a* the factor taking into account both the efficiency of the gamma counter for ^{67}Ga and the abundance of the gamma ray used for counting. The total number of decays accumulated in nucleus during the incubation was estimated using the following calculations and assumptions: 1) the area under the curve, expressed as the number of decays occurring in the nucleus during the incubation with predefined concentrations of ^{67}Ga-NOTA-MNT, was calculated from the nuclear kinetics experiment data (0–24 h) and 2) it was assumed that the percentage of decays that occurred per nucleus is constant over the concentration range of ^{67}Ga-NOTA-MNT concentrations used in the cytotoxicity studies.

2.8 Dosimetry calculations

The estimated radiation absorbed doses in Gy delivered to the cell nuclei were calculated based on standard MIRD formalism that utilizes cellular S values to determine self absorbed dose per unit cumulated activity incorporated into different cell compartments [6]. The dose to the cell nucleus was calculated based on the following equation:

$$D = C^{*}S(N \leftarrow C_{Y}) + N^{*}S(N \leftarrow N)$$

where C are the decays/cell and N are the decays/nucleus, and $S(N \leftarrow C_Y)$ and $S(N \leftarrow N)$ are the cellular S values for dose delivered to the cell nucleus from decays originating in the cytoplasm and cell nucleus, respectively. Because these S values are dependent on the geometry of the cell, fluorescence microscopy was utilized to measure the size of approximately 100 A431 cells, which were found to have cellular and nuclear radii of 10.0 ± 0.9 μm and 6.7 ± 0.2 μm, respectively. Published S values [6] for ^{67}Ga for cells with these dimensions were utilized in these calculations.

2.9 Statistical analysis

The acquired data were analyzed for statistical significance using the Graph Pad Prism Version 5.01 software. Each data point on the plots represents either the mean of the values obtained from independent experiments or the mean of the values of triplicates for each point, with error bars indicating the Standard Deviation (± S.D.).

3. Results

3.1 Conjugation of MNT with pSCN-Bn-NOTA

Analysis of MNT and its NOTA conjugates by SDS PAGE revealed a single band consistent with the molecular weight of MNT (76.3 kDa). MALDI-MS analysis of MNT and its NOTA conjugates was performed to evaluate the C/B ratio, which was determined to be in the range of 1 to 2.5. Similar C/B ratios were determined for NOTA-BSA and NOTA-hEGF.

3.2 Radiolabeling of NOTA-MNT with ^{67}Ga

Because the isoelectric point of the MNT construct is 5.7, it is soluble in two pH windows—below 3.5 and above 7.4. As expected, precipitation of NOTA-MNT was observed when labeling reactions were performed at pH 4.5–5.0 where ^{67}Ga is generally performed. Solubilization of NOTA-MNT was achieved by the addition of DMSO or SDS at a final concentration of 5% (v/v). With DMSO as a solubilizing agent, labeling yields of about 63% were obtained; however, the majority of the ^{67}Ga activity could not be removed from the walls of the Eppendorf tube. Use of SDS as the solubilizing agent did not result in successful labeling of NOTA-MNT. In order to confirm the effects of conjugate solubility, NOTA-BSA, which is soluble at pH 4.5–5.0, was labeled with ^{67}Ga under these conditions, but without the presence of DMSO or SDS, and excellent labeling yields were obtained. The feasibility of labeling NOTA-MNT as a heterogeneous mixture at pH 5.0 was investigated. The premise was that if higher labeling yields resulted, the mixture could be solubilized in pH 8 phosphate buffer and then purified by gel filtration. The reactions were done at 37°C

for 1 and 2 h, and there was a 12-fold increase in labeling yield at pH 5 compared to those obtained at pH 3 and 8. Increasing the reaction time increased labeling yield only at pH 3. Having optimized the pH, temperature and duration of incubation, the effect of activity concentration on labeling yield was determined. The radiochemical yield determined by ITLC before and after PD-10 purification, was more than 90%. The radiochemical yield, expressed as the percent of total radioactivity loaded onto a gel filtration column eluting in the protein-associated fractions, increased as a function of initial radioactivity concentration up to 16 mCi/mL (83.6 ± 8.3% yield), but decreased thereafter (Fig. 1A), possibly due to radiolytic effects. Methanol precipitation of pooled protein fractions indicated no difference in the fraction of ^{67}Ga remaining protein associated as a function of activity concentration, suggesting radiation-mediated loss of label from the MNT conjugate was not a factor (Fig. 1A). As expected, the specific activity increased with increasing radioactivity concentration until 16 mCi/mL where a maximum value of 2.0 ± 0.2 Ci/μmol (~26 mCi/mg) was obtained (Fig. 1B). SDS-PAGE analysis of the ^{67}Ga-NOTA-MNT conjugate indicated that 80% and 10–20% of the ^{67}Ga was present in bands with molecular weights of 75 and 150 kDa, presumably reflecting the presence of monomeric and dimeric conjugates, respectively.

3.3 Uptake and washout kinetics

The uptake and washout kinetics of ^{67}Ga-NOTA-MNT was evaluated using the EGFR-expressing A431 cell line. Intracellular radioactivity increased steadily over time and began to plateau at 24 h (Fig 2A). Membrane bound ^{67}Ga activity was considerably lower and remained relatively stable over time. The total cellular uptake at 24 h was 30.1 ± 4.6% of input radioactivity. Considering the half-life of ^{67}Ga, and the uptake kinetics, a 24 h incubation period was deemed suitable for the washout kinetics and cytotoxicity studies. Washout of radioactivity from A431 cells was slow (Fig 2B), with 76.9 ± 3.5 % and 52.4 ± 0.9% of initially bound radioactivity retained on/in the cells and internalized after 24 h, respectively.

These uptake and washout kinetic data were fitted to exponential functions. Uptake kinetics were fit to $y = y_{max}*(1-e^{-kx})$ yielding equation 1: $\mathbf{cpm_1}(t)=6.821(1-\mathrm{e}^{-0.001193\mathrm{t}})$, where t is the incubation time (R^2=0.99). Washout kinetics were fit with the exponential equation $y = a_1e^{k1x} + a_2e^{k2x}$ yielding equation 2: $\mathbf{cpm_2}(t)=2.095\mathrm{e}^{-0.0001744\mathrm{t}}+1.420\mathrm{e}^{-0.004995\mathrm{t}}$, where t is the incubation time (R^2=0.92). In order to obtain the **$cpm_1(t)$** and **$cpm_2(t)$** integral functions for each concentration of ^{67}Ga-NOTA-MNT used in the cytotoxicity experiments, we assumed that the shape of kinetics functions was not dependent on ^{67}Ga-$(NOTA)_n$-MNT concentration. Based on this assumption, we calculated the $y_{max}(c)$ from the internalized radioactivity for a 24-h incubation, and derived the respective **$cpm_1(t)$** equations at each concentration. The **$cpm_2(t)$** integral was calculated from the concentration used for the washout kinetics at 24 h.

3.4 In vitro nuclear kinetics

Because of the short range of ^{67}Ga Auger electrons, their cytotoxicity is highest when localized in the cell nucleus. For this reason, the kinetics of ^{67}Ga nuclear translocation was determined after incubation of A431 cells with ^{67}Ga-NOTA-MNT. At 1 h, 55.5 ± 3.0% of

the total intracellular radioactivity was present in the nuclei indicating that the nuclear translocalization of ^{67}Ga-NOTA-MNT was rapid (Fig. 3A). The fraction of intracellular activity found in the nucleus decreased to 15.4 ± 1.7% at 4 h and 7.3 ± 1.0% at 24 h. The absolute levels of radioactivity present inside the cells and the cell nuclei as a function of time are shown in Fig 3B. At 1 h, 0.295 ± 0.017 cpm/cell nucleus was observed, remaining relatively constant at near this level through 4 h, declining to about 0.15 cpm/cell nucleus at 8 and 24 h.

3.5 Cytotoxicity measurements

The clonogenic survival of A431 cells after treatment for 24 h with increasing activity concentrations of ^{67}Ga-NOTA-MNT, and as controls for nonspecific cytotoxicity, ^{67}Ga-EDTA and ^{67}Ga-NOTA-BSA, is shown in Fig. 4A. The radioactive concentrations required to reduce survival to 37% (A_{37}), and to 10% (A_{10}) were determined by regression analysis and are presented in Table 1. The A_{37} value for ^{67}Ga-NOTA-MNT was 5.4×10^6 dpm/well while this degree of cell killing required 17 and 385 times more radioactivity for ^{67}Ga-NOTA-BSA and ^{67}Ga-EDTA, respectively, demonstrating a high degree of enhancement in cytotoxicity for the EGFR-specific ^{67}Ga-NOTA-MNT conjugate.

The percent of protein-associated activity for ^{67}Ga-NOTA-MNT and ^{67}Ga-NOTA-BSA in the cell culture supernatants from the cytotoxicity experiments was determined by methanol precipitation (Fig. 5A). These results demonstrate that the lower cytotoxicity of ^{67}Ga-NOTA-BSA compared with ^{67}Ga-NOTA-MNT cannot be explained by differences in stability of the two compounds under assay conditions. In addition, the internalized and membrane-bound radioactivity of both ^{67}Ga-labeled proteins was also determined in the cytotoxic assay (Fig. 5B) and <0.5% of the total added activity was present inside the cells for ^{67}Ga-NOTA-BSA at all concentrations in marked contrast to the orders of magnitude higher intracellular uptake observed with ^{67}Ga-NOTA-MNT.

In order to determine a possible role of the intracellular routing modules present in the MNT construct in enhancing cytotoxicity, the cytotoxic effectiveness of ^{67}Ga-NOTA-MNT was compared to that of an EGFR-targeted agent lacking these functions, ^{67}Ga-NOTA-hEGF, on both A431 (Fig. 4A) and WTT (Fig. 4B) cells. On A431 cells, 13 and 18 times more radioactivity would be required to reduce survival to 37% and 10% levels with ^{67}Ga-NOTA-hEGF (Table 1). Likewise, A_{37} and A_{10} values were 72 and 18 times higher for ^{67}Ga-NOTA-hEGF compared with ^{67}Ga-NOTA-MNT on WTT glioma cells. These results suggest that factors in addition to EGFR targeting contribute to the cytotoxic effectiveness of ^{67}Ga-NOTA-MNT.

3.6 Dosimetry

The calculated number of decays per cell and decays per cell nucleus required to reduce survival to 37% (N_{37}) and 10% (N_{10}) for A431 cells are presented in Table 2. In order to relate survival to radiation dose delivered to the cell nucleus, contributions from ^{67}Ga decaying in the cytoplasm and the cell nucleus were considered. Calculations were based on the accumulated activity at the beginning of the clonogenic assay and not over the time course of the assay. The survival fraction as a function of the calculated Gy dose delivered

to the nucleus per A431 cell from ^{67}Ga-NOTA-MNT is presented in Fig. 6. The absorbed doses for 37% and 10% cell survival were D_{37} =9 Gy and D_{10} = 21 Gy.

4. Discussion

Having established that MNT-mediated nuclear delivery of short-range therapeutics such as photosensitizers [12,13,16], and α-particle-emitting radionuclides [7] increased their therapeutic effect, we hypothesized that MNT also could be a useful carrier for delivering ultra-short range Auger electron-emitting radionuclides to the cell nucleus. Although previous work demonstrated proof of concept with the prototypical Auger electron-emitting radionuclide ^{125}I, its 60-day half-life is not ideal for targeted radiotherapy application in patients [21]. Gallium-67 was selected for investigation in the current study as a potentially more clinically translatable alternative based on: a) its 3.26-d half-live, which is more compatible with the intracellular kinetics observed with MNT [14]; b) emission of 4.7 Auger and Coster-Kronig electrons per decay [22]; c) availability at a reasonable cost; and d) wealth of clinical experience with ^{67}Ga as an imaging agent.

NOTA was chosen for labeling MNT with ^{67}Ga because it has a high complex stability constant for Ga(III), which is also reflected in the remarkable acid stability of the complex [15]. Unlike the case with other proteins, labeling MNT with ^{67}Ga was challenging, because of its insolubility in the pH range of 4.5–5.0, which is optimal for labeling with trivalent radiometals such as ^{67}Ga [23]. For this reason, we investigated several approaches in order to achieve high radiolabeling yield and specific activity. Prelabeling, where metal complexation is performed first followed by a conjugation step, has been used successfully in the past [24,25,26] to circumvent difficulties created by biomolecule incompatibility with conditions required for effective radiolabeling. However, only limited amounts of MNT were available, which precluded the use of this approach except at activity levels lower than those required for the cytotoxicity assays. Moreover, the need for an excess of MNT to achieve acceptable radiolabeling yields would compromise specific activity. The feasibility of radiolabeling the NOTA-MNT conjugate was pH windows 2.5–3.5 and 7.5–8.5, and gave radiolabeling yields of <1–2%. Next, we tried radiolabeling MNT at pH 5.0 with solubilization by DMSO or SDS; however, this approach also was futile. Eventually, we were successful in radiolabeling NOTA-MNT in >90% yield as a heterogeneous mixture at pH 5.0 with subsequent solubilization by buffer/DMSO solution. The maximum specific activity achieved (2.0 Ci/μmol, ~26 mCi/mg) was comparable [24] or even higher [27] to those reported elsewhere. The observed plateau of specific activity might be due to the limited number of chelators present in the MNT.

The retention of radioactivity in tumor cells following binding and internalization of a radiolabeled receptor-avid protein to a particular receptor depends on multiple factors including the nature of the protein, the radiolabeled prosthetic group and the properties of the radionuclide [28]. In past studies with a variety of receptor-targeted biomolecules, SGMIB was shown to be one of the best residualizing agents for trapping radioiodine in tumor cells [29]. With a monoclonal antibody specific for mutant EGFR, SGMIB provided similar tumor cell retention *in vitro* for up to 8 h compared to all but one radiometal labeled antibody conjugates studied; however, at 24 h, the ^{177}Lu/^{125}I retention ratio increased from

1.5 to 3.0 [17]. In the uptake experiment, the intracellular retention of radioactivity (normalized per 10^6 cells) by EGFR-expressing A431cells was higher as early as 2 h after exposure to ^{67}Ga-NOTA-MNT than that observed previously with [^{125}I]SGMIB-MNT [14], with a 2.5-fold difference seen at 24 h (^{67}Ga-NOTA-MNT, 75.0 ± 1.8%; [^{125}I]SGMIB-MNT, 29.9 ±3.4%, Fig. 7). Likewise, in the washout study, about 50% of the initially bound radioactivity from ^{67}Ga-NOTA-MNT remained internalized at 24 h, representing a twofold advantage compared to [^{125}I]SGMIB-MNT. Although *in vitro* catabolism experiments were beyond the scope of this study, these results suggest more efficient trapping of labeled catabolites such as ^{67}Ga-NOTA or its amino acid adduct compared with those generated after [^{125}I]SGMIB labeling [30].

Given the potential therapeutic advantage for Auger electron emission in close proximity to DNA, the dynamics of nuclear translocation of ^{67}Ga was determined. About 56% of the internalized ^{67}Ga-NOTA-MNT was found in the cell nuclei of A431 cells after 1 h, in good agreement with the results obtained with [^{125}I]SGMIB-MNT [14]; the washout of ^{67}Ga activity from cell nuclei occurred at a 3 times slower rate, with nuclear activity declining 40% and 14% at 3 h for ^{125}I and ^{67}Ga, respectively, also in agreement with the overall washout rate of both compounds. It is worth noting that the same tendency for significant washout of radioactivity from the nucleus over time was reported for an ^{111}In-labeled anti-EGFR antibody-NLS conjugate [31]. Although the reasons for this behavior are not known, factors that could play a role include differences in the action of proteasomes in the cell nucleus and the cytoplasm [32], binding of labeled catabolites to nuclear elements, and transport across nuclear pores. Nonetheless, the fact that more than half of the internalized radioactivity was present in cell nuclei at 1 h suggests efficient escape of MNT molecules from lysosomes, most likely facilitated by its DTox module.

In assessing the *in vitro* cytotoxicity of targeted radiotherapeutics, two important parameters are the specificity and potency of the therapeutic effect. In addition to its subcellular range Auger electron emissions, ^{67}Ga also emits several gamma rays and conversion electrons with multicellular range [22]. Thus, some degree of nonspecific killing would be expected to occur in our clonogenic assays, particularly when the 24 h incubation period is considered. In the current study, the cytotoxic effectiveness of ^{67}Ga-NOTA-MNT on A431 cells was demonstrated to be 17 higher than that of ^{67}Ga-NOTA-BSA. In comparison, the cytotoxicity of [^{125}I]SGMIB-MNT was more than 1,000 higher than that of [^{125}I]iodoBSA on the same cell line, consistent with the considerably lower fraction of emissions of greater than 1 μm tissue range in the ^{125}I vs. ^{67}Ga decay scheme. An additional factor that could account for the lower degree of specific killing is that a greater fraction of ^{67}Ga decays occurred when nonspecific binding was most likely to occur.

With regard to the evaluating the cytotoxic effectiveness of ^{67}Ga-NOTA-MNT, cell killing could be achieved on two EGFR-expressing cancer cell lines with more than 15 times less activity than required with ^{67}Ga-NOTA-hEGF. The fact that these molecules target the same receptor, were evaluated on the same cell lines and using the same assay format suggests that the additional functions built into the MNT structure, namely endosome escape and nuclear import, contribute to its utility as a carrier for ^{67}Ga. A similarly enhanced cytotoxicity was observed for [^{125}I]SGMIB-MNT compared with [^{125}I]SGMIB-hEGF;

however, the number of molecules required to achieve a similar level of cell killing was higher for the ^{67}Ga compound compared with its ^{125}I-labeled equivalent. For example, the number of ^{67}Ga-NOTA-MNT molecules per cell required to reduce survival of A431 cells to 37% was 28,600 per cell, about 9.5 times higher than required with [^{125}I]SGMIB-MNT [14]. This is not unexpected given that the total number of <0.1 μm tissue-range Auger electrons is almost 6 times higher for ^{125}I [22]. Although the number of ^{67}Ga atoms required per molecule is relatively high, this does not discourage further evaluation of ^{67}Ga-NOTA-MNT as a targeted therapeutic because this represents only about 1% receptor occupancy.

The therapeutic potential of several ^{67}Ga-labeled compounds has been described [2, 27, 32–34]; however, comparison to those reported herein must be done with caution because differences in factors such as cell sensitivity, geometry, assay design and stability of the labeled agent could complicate interpretation. Nonetheless, the calculated radiation absorbed doses of ^{67}Ga-NOTA-MNT required to reduce survival to 37% and 10%, 8 and 18 Gy, respectively, were in good agreement to those reported previously for several internalizing antibodies labeled with ^{67}Ga [33–35].

The subcellular range of Auger electrons is an attractive feature for minimizing collateral damage to normal tissues adjacent to tumor. Conversely, the absence of a substantive physical crossfire effect such as that associated with a long-range β-particle could be challenging in situations where heterogeneous delivery of the targeted radiotherapeutic to the malignant cell population can occur. Fortuitously, this problem may be ameliorated by the radiation-induced biological bystander effect (RIBBE), a process that results in the killing of cells not directly exposed to radiation [36]. Because the RIBBE is most frequently observed at low dose rates and low radiation doses [37], it is of potential relevance to targeted radiotherapy where these conditions frequently occur. Although the mechanisms responsible for the RIBBE are not understood completely, Auger electron-emitting radiopharmaceuticals have been shown to exhibit RIBBE-mediated destruction of cancer cells in both in vitro and in vivo studies [38, 39]. The extent to which RIBBE can be harnessed to increase the therapeutic effectiveness of ^{67}Ga-NOTA-MNT will be evaluated in future studies.

5. Conclusion

Despite its incompatibility with typical ^{67}Ga labeling conditions, we have demonstrated that the EGFR-specific and nuclear-targeted chimeric biomolecule MNT can be efficiently labeled with Auger electron-emitting ^{67}Ga using NOTA. The ^{67}Ga-NOTA-MNT conjugate was shown to undergo rapid internalization and translocation to the cell nucleus of EGFR-expressing cancer cells, and was considerably more cytotoxic *in vitro* than negative controls and ^{67}Ga-NOTA-hEGF. Taken together, these results confirm the potential of MNT as a platform for the development of Auger electron emitting targeted radiotherapeutics with ^{67}Ga, a radionuclide with properties appropriate for clinical application. With that goal in mind, we are currently evaluating the therapeutic efficacy of ^{67}Ga-NOTA-MNT in athymic mice bearing EGFR-expressing human glioma xenografts.

Acknowledgments

This work was supported in part by National Institutes of Health Grants CA42324 and NS20023, RF State Contracts 16.512.12.2004, and 13411.1008799.13.135, and RFBR grant number 10-04-01037-a.

References

1. Buchegger F, Perillo-Adamer F, Dupertuis YM, Delaloye AB. Auger radiation targeted into DNA: a therapy perspective. Eur J Nucl Med Mol Imaging. 2006; 33:1352–63. [PubMed: 16896663]
2. Cornelissen B, Vallis KA. Targeting the Nucleus: an overview of Auger-Electron Radionuclide therapy. Current Drug Discovery Technologies. 2010; 7:263–79. [PubMed: 21034408]
3. Pouget JP, Santoro L, Raymond L, Chouin N, Bardiès M, Bascoul-Mollevi C, et al. Cell membrane is a more sensitive target than cytoplasm to dense ionization produced by Auger electrons. Radiat Res. 2008; 170:192–200. [PubMed: 18666820]
4. Reilly RM, Kiarash R, Cameron RG, Porlier N, Sandhu J, Hill RP, et al. ^{111}In-labeled EGF is selectively radiotoxic to human breast cancer cells overexpressing EGFR. J Nucl Med. 2000; 41:429–38. [PubMed: 10716315]
5. Hofer KG, Harris CR, Smith MJ. Radiotoxicity of intracellular Ga-67, I-125 and H-3: nuclear versus cytoplasmic radiation effects in murine L1210 leukemia cells. Int J Radiat Biol Relat Stud Phys Chem Med. 1975; 28:225–41. [PubMed: 1081511]
6. Goddu, SM.; Howell, RW.; Bouchet, LG.; Bolch, WE.; Rao, DV. MIRD cellular S values. Reston, V.A: Society of Nuclear Medicine; 1997.
7. Rosenkranz AA, Vaidyanathan G, Pozzi OR, Lunin VG, Zalutsky MR, Sobolev AS. Engineered modular recombinant transporters: application of new platform for targeted radiotherapeutic agents to α-particle emitting ^{211}At. Int J Radiation Oncology Biol Phys. 2008; 72:193–200.
8. Chen P, Wang J, Hope K, Jin L, Dick J, Cameron R, et al. Nuclear localizing sequence promote nuclear translocation and enhance the radiotoxicity of the ant-CD33 monoclonal antibody HUM195 labeled with ^{111}In in human myeloid leukemia cells. J Nucl Med. 2006; 47:827–36. [PubMed: 16644753]
9. Costantini D, Chan C, Cai Z, Vallis KA, Reilly RM. ^{111}In–labeled trastuzumab (Herceptin) modified with nuclear localization sequence (NLS): an Auger electron-emitting radiotherapeutic agent for HER2/neu-amplified breast cancer. J Nucl Med. 2007; 48:1357–68. [PubMed: 17631548]
10. Yarden Y, Sliwkowski MX. Untangling the ErbB signaling network. Nat Rev Mol Cell Biol. 2001; 2:127–137. [PubMed: 11252954]
11. Hatanpaa KJ, Burma S, Zhao D, Habib AA. Epidermal growth factor receptor in glioma: signal transduction, neuropathology, imaging, and radioresistance. Neoplasia. 2010; 12:675–84. [PubMed: 20824044]
12. Rosenkranz AA, Lunin VG, Gulak PV, Sergienko OV, Shumiantseva MA, Voronina OL, et al. Recombinant modular transporters for cell-specific nuclear delivery of locally acting drugs enhance photosensitizer activity. FASEB Journal. 2003; 17:1121–1123. [PubMed: 12692081]
13. Slastnikova TA, Rosenkranz AA, Gulak PV, Schiffelers RM, Lupanova TN, Khramtsov YV, et al. Modular nanotransporters: a multipurpose in vivo working platform for targeted drug delivery. Int J Nanomedicine. 2012; 7:467–82. [PubMed: 22346349]
14. Slastnikova TA, Koumarianou E, Rosenkranz AA, Vaidyanathan G, Lupanova TN, Sobolev AS, et al. Modular nanotransporters: a versatile approach for enhancing nuclear delivery and cytotoxicity of Auger electron emitting ^{125}I. EJNMMI Research. 2012; 2:59–69. [PubMed: 23107475]
15. Lee J, Garmestani K, Wu C, Brechbiel MW, Chang HK, Choi CW, et al. In vitro and in vivo evaluation of structure –stability relationship of ^{111}In- and ^{67}Ga-labelled antibody via 1B4M or C-NOTA chelates. Nucl Med Biol. 1997; 24:225–30. [PubMed: 9228656]
16. Gilyazova DG, Rosenkranz AA, Gulak PV, Lunin VG, Sergienko OV, Khramtsov YV, et al. Targeting cancer cells by novel engineered modular transporters. Cancer Res. 2006; 66:10534–40. [PubMed: 17079476]

17. Hens M, Vaidyanathan G, Zhao XG, Bigner DD, Zalutsky MR. Anti-EGFRvIII monoclonal antibody armed with ^{177}Lu: in vivo comparison of macrocyclic and acyclic ligands. Nucl Med Biol. 2010; 37:741–50. [PubMed: 20870149]
18. Reist CJ, Foulon CF, Alston K, Bigner DD, Zalutsky MR. Astatine-211 labeling of internalizing anti-EGFRvIII monoclonal antibody using N-succinimidyl 5-[^{211}At]astato-3-pyridinecarboxylate. Nucl Med Biol. 1999; 26:405–11. [PubMed: 10382844]
19. Zalutsky MR, Boskovitz A, Kuan C-T, Pegram CN, Ayriss J, Wikstrand CJ, et al. Radioimmunotargeting of malignant glioma by monoclonal antibody D2C7 reactive against both wild-type and variant III mutant epidermal growth factor receptors. Nucl Med Biol. 2012; 39:23–34. [PubMed: 21958852]
20. Lo HW, Hsu S-C, Wei Y, Bartolomeusx G, Shih J-Y, Hung MC. Nuclear interaction of EGFR and STAT3 in the activation of iNOS/NO pathway. Cancer Cell. 2005; 6:575–89. [PubMed: 15950906]
21. Karagiannis TC. Antibody – based cancer treatment with ultra-short range Auger electron-emitting radionuclides: Dual receptor and DNA targeting strategies. Hell J Nucl Med. 2007; 10:155–9. [PubMed: 18084655]
22. Howell RW. Radiation spectra for Auger-electron emitting radionuclides: report No. 2 of AAPM. Nuclear Medicine Task Group No. 6. Med Phys. 1992; 19:1371–83. [PubMed: 1461199]
23. Heeg MJ, Jurisson SS. The role of inorganic chemistry in the development of radiometal agents for cancer therapy. Acc Chem Res. 1993; 32:1050–60.
24. Li M, Meares CF, Salako Q, Kukis DL, Zhong G-R, Miers L, et al. Prelabeling of chimeric monoclonal antibody L6 with ^{90}Yttrium- and ^{111}Indium-1,4,7,10-tetraazacyclododecane-N, N′, N″, N‴-tetraacetic acid (DOTA). Chelates for radioimmunodiagnosis and therapy. Cancer Research. 1995; 55(Suppl):5726s–5728s. [PubMed: 7493335]
25. Wangler C, Schirrmacher R, Bertenstein P, Wangler B. Simple and convenient radiolabeling of proteins using a prelabeling-approach with thiol-DOTA. Bioorg Med Chem Letters. 2009; 19:1926–9.
26. Bauwens M, De Saint-Hubert M, Devos E, Deckers N, Reutelingsperger C, Mortelmans L, et al. Site-specific ^{68}Ga-labeled Annexin A5 as a PET imaging agent for apoptosis. Nucl Med Biol. 2011; 38:381–92. [PubMed: 21492787]
27. Govindan SV, Michel RB, Griffiths GL, Goldenberg DM, Mattes MJ. Deferoxamine as a chelator for ^{67}Ga in the preparation of antibody conjugates. Nucl Med Biol. 2005; 32:513–9. [PubMed: 15982582]
28. Stein R, Govindan SV, Mattes MJ, Chen S, Reed L, Newsome G, et al. Improved iodine radiolabels for monoclonal antibody therapy. Cancer Res. 2003; 63:111–118. [PubMed: 12517786]
29. Vaidyanathan G, Zalutsky MR. Synthesis of N-succinimidyl 4-guanidinomethyl-3-[*I]iodobenzoate: a radio-iodination agent for labeling internalizing proteins and peptides. Nature Protocols. 2007; 2:282–6.
30. Vaidyanathan G, Affleck DJ, Li J, Welsh P, Zalutsky MR. A polar substituent-containing acylation agent for the radioiodination of internalizing monoclonal antibodies: N-succinimidyl 4-guanidinomethyl-3-[131I]iodobenzoate ([^{131}I]SGMIB). Bioconjug Chem. 2001; 12:428–38. [PubMed: 11353542]
31. Fasih A, Fonge H, Cai Z, Leyton JV, Tikhomirov I, Done SJ, et al. ^{111}In-Bn-DTPA-nimotuzumab with/without modification with nuclear translocation sequence (NLS) peptides: an Auger electron-emitting radioimmunotherapeutic agent for EGFR-positive and trastuzumab (Herceptin)-resistant breast cancer. Breast Cancer Res Treat. 2012; 135:189–200. [PubMed: 22736376]
32. Reits EA, Benham AM, Plougastel B, Neefjes J, Trowsdale J. Dynamics of proteasome distribution in living cells. EMBO J. 1997; 16:6087–94. [PubMed: 9321388]
33. Govindan SV, Goldenberg DM, Elsarma SE, Griffiths GL, Ong GL, Brechbiel MW, et al. Radionuclides linked to CD74 antibody as therapeutic agents for B-Cell lymphoma: comparison of Auger electron emitters with β-particle emitters. J Nucl Med. 2000; 41:2089–97. [PubMed: 11138697]

34. Shih LB, Thorpe SR, Griffiths GL, Diril H, Ong GL, Hansen HJ, et al. The processing and fate of antibodies and their radiolabels bound to the surface of tumor cells in vitro: a comparison of nine radiolabels. J Nucl Med. 1994; 35:899–908. [PubMed: 8176479]

35. Michel RB, Brechbiel MW, Mattes MJ. A comparison of 4 radionuclides conjugates to Antibodies for single-cell kill. J Nucl Med. 2003; 44:632–40. [PubMed: 12679410]

36. Seymour CB, Mothersill C. Relative contribution and targeted cell killing to the low-dose region of the radiation dose-response curve. Radiat Res. 2000; 153:508–511. [PubMed: 10790270]

37. Little JB, Azzam EI de Toledo SM, Nagasawa H. Bystander effects: intracellular transmission of radiation damage signals. Radiat Prot Dosimetry. 2002; 99:159–62. [PubMed: 12194273]

38. Boyd M, Ross SC, Dorrens J, Fullerton NE, Tan KW, Zalutsky MR, et al. Radiation-induced biological bystander effect elicited in vitro by radiopharmaceuticals labeled with α-, β-and Auger elstron-emitting radionuclides. J Nucl Med. 2006; 47:1007–15. [PubMed: 16741311]

39. Xue LY, Butler NJ, Makrigiorgos GM, Adelstein SJ, Kassis AI. Bystander effect produced by radiolabeled tumor cells *in vivo*. Proc Natl Acad Sci USA. 2002; 99:13765–70. [PubMed: 12368480]

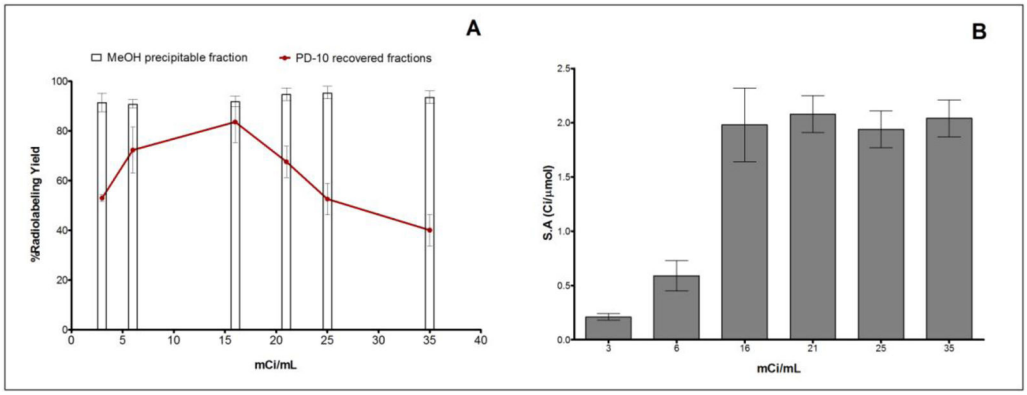

Fig. 1.

(A) Radiochemical yield of ^{67}Ga-NOTA-MNT as a function of initial ^{67}Ga concentration. Line plot shows the percent of total activity loaded onto PD-10 column recovered in protein fractions, while bars indicate percentage of radioactivity in these fractions precipitable by methanol. (B) Specific activity (Ci/μmol) of ^{67}Ga-NOTA-MNT as a function of initial ^{67}Ga concentration. Reactions were conducted by incubating 100 μg of NOTA-MNT with 3–35 mCi/mL ^{67}Ga at 37°C for 1 h at pH 5. ^{67}Ga-NOTA-MNT was solubilized by addition of 5% DMSO in phosphate buffer, pH 8.5 at the end of incubation. Error bars represent standard deviation of 3 independent experiments.

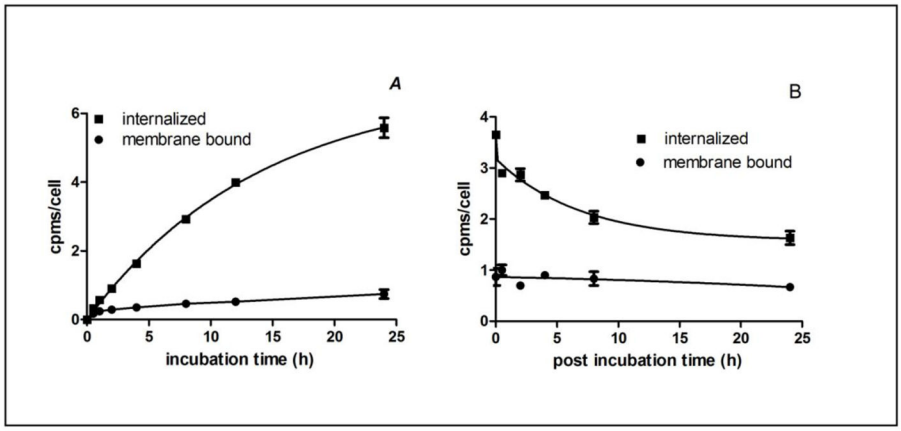

Fig. 2.

Uptake (A) and washout (B) kinetics of ^{67}Ga-NOTA-MNT on A431 human epidermoid carcinoma cells. In the uptake study, cells were incubated with tracer and internalized radioactivity was determined as a function of time. To determine washout kinetics, cells were incubated with ^{67}Ga-NOTA-MNT for 24 h, washed and then internalized radioactivity was determined. Error bars represent the standard deviation of 2 independent experiments.

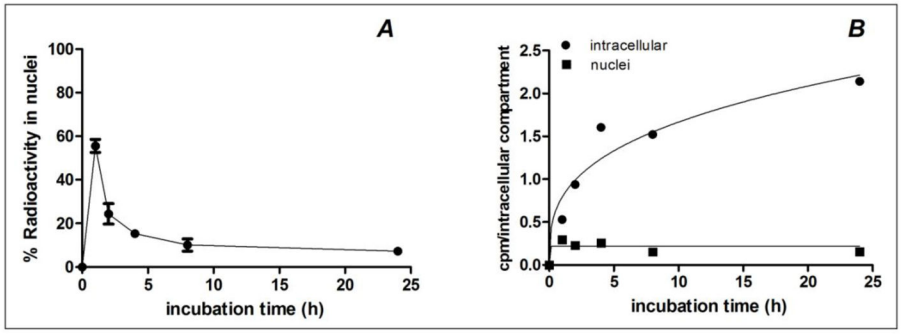

Fig. 3.

Representative graph of (A) nuclear uptake kinetics as percent of internalized radioactivity and of (B) nuclear and total intracellular uptake of ^{67}Ga-NOTA-MNT by A431 human epidermoid carcinoma cells. Error bars represent the standard deviation of triplicates for each time point.

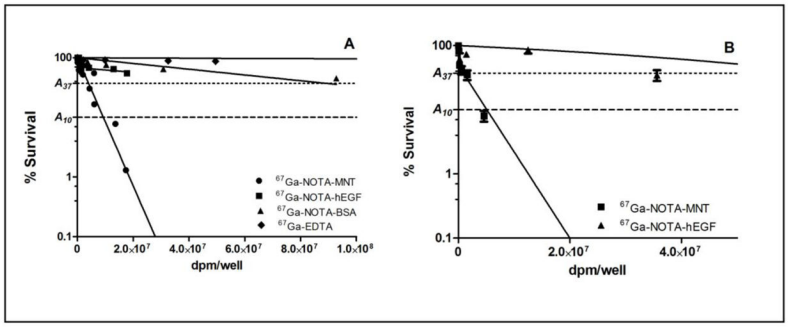

Fig. 4.

Clonogenic survival of EGFR-expressing (A) A431 human epidermoid carcinoma cells after exposure for 24 h to varying activity concentrations of ^{67}Ga-NOTA-MNT, ^{67}Ga-NOTA-hEGF, ^{67}Ga-NOTA-BSA and ^{67}Ga-EDTA, and (B) WTT human glioblastoma cells after exposure for 24 h to varying activity concentrations of ^{67}Ga-NOTA-MNT and ^{67}Ga-NOTA-hEGF. Error bars represent the standard deviation of 2 independent experiments.

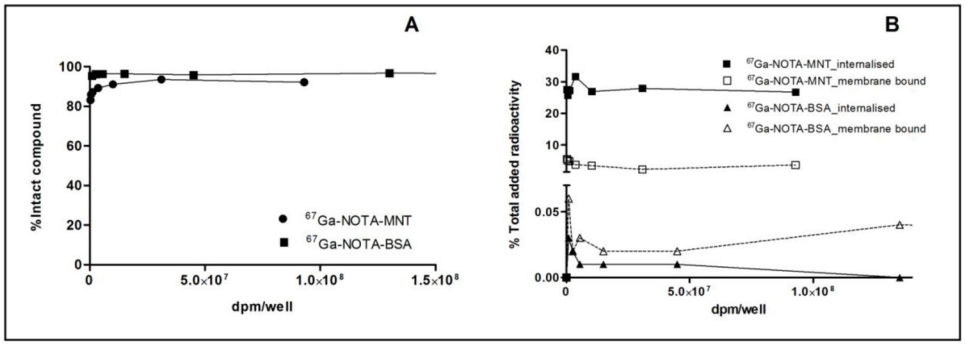

Fig. 5.

Representative graphs of (A) percent of ^{67}Ga activity in the cell culture media that is protein associated, and (B) membrane bound and internalized ^{67}Ga activity, expressed as percent of total added radioactivity for ^{67}Ga-NOTA-MNT and ^{67}Ga-NOTA-BSA after exposure of cells under cytotoxicity assay conditions. Error bars represent the standard deviation of triplicates for each point.

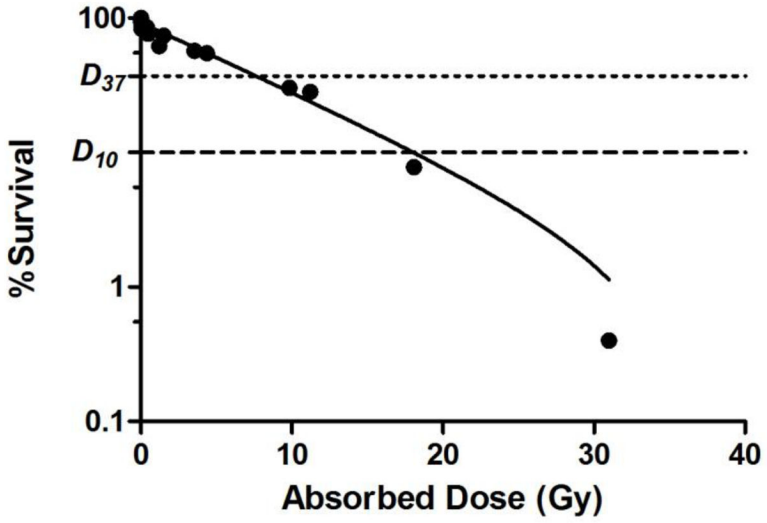

Fig. 6.

Clonogenic survival *vs*. radiation dose (Gy) delivered to nuclei of A431 human epidermoid carcinoma cells after 24-h exposure to of ^{67}Ga-NOTA-MNT.

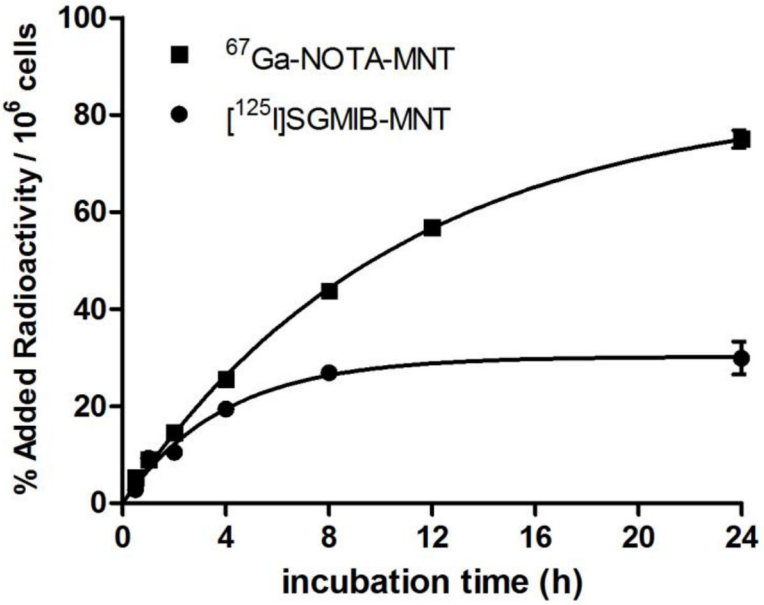

Fig. 7.

Comparison of intracellular localization kinetics of ^{67}Ga-NOTA-MNT to [^{125}I]SGMIB-MNT [14] in A431 cells expressed as percent of added radioactivity per 10^6 cells. Error bars represent the standard deviation of triplicates for each time point.

Table 1

Cytotoxicity of ^{67}Ga-NOTA-MNT compared with other ^{67}Ga-labeled compounds on A431 epidermoid carcinoma cells and WTT human glioblastoma cells.

Cell Line	^{67}Ga Compound	A_{37} (dpm × 10^{-6}) (*compound/MNT*)[a]	A_{10} (dpm × 10^{-6}) (*compound/MNT*)[a]
A431 cells	NOTA-MNT	5.4	12.4
	NOTA-hEGF	69.8 *(13)*	218.6 *(18)*
	NOTA-BSA	89.5 *(17)*	207.3 *(17)*
	EDTA	2079.5 *(385)*	4816.1 *(388)*
WTT cells	NOTA-MNT	0.9	5.1
	NOTA-hEGF	64.8 *(72)*	92.6 *(18)*

[a]Values in parentheses are ratios of A_{37} and A_{10} values of compounds to values for ^{67}Ga-NOTA-MNT.

Table 2

Cytotoxicity of ^{67}Ga-NOTA-MNT compared with [^{125}I]SGMIB-MNT [14] on A431 human epidermoid cells expressed as decays per cell and per cell nucleus.

Compound	N_{37} (decays/cell)	N_{37} (decays/cell nucleus)	N_{10} (decays/cell)	N_{10} (decays/cell nucleus)
^{67}Ga-NOTA-MNT	28,600	9,700	66,300	22,400
[^{125}I]SGMIB-MNT	3,000	300	7,100	800